Profiling substrate specificity of two series of phenethylamine analogs at monoamine oxidase A and B.

Egon Heuson, Morten Storgaard, Tri H. V. Huynh, Franck Charmantray, Thierry Gefflaut, Lennart Bunch

Organic & Biomolecular Chemistry

PAPER

View Article Online
View Journal | View Issue

Cite this: *Org. Biomol. Chem.*, 2014, **12**, 8689

Profiling substrate specificity of two series of phenethylamine analogs at monoamine oxidase A and B†

Egon Heuson,[a,b] Morten Storgaard,[c] Tri H. V. Huynh,[c] Franck Charmantray,[a,b] Thierry Gefflaut*[a,b] and Lennart Bunch*[c]

Received 2nd July 2014,
Accepted 11th September 2014

DOI: 10.1039/c4ob01377h

www.rsc.org/obc

The membrane bound enzyme *monoamine oxidase* exist in two splice variants designated A and B (MAO-A and MAO-B) and are key players in the oxidative metabolism of monoamines in mammalians. Despite their importance and being a prevalent target for the development of inhibitors as drugs, no systematic study of substrate specificity has been reported. In this study we present a systematic study of the MAO-A and MAO-B substrate specificity profile by probing two series of phenethylamine analogs. K_m and k_{cat} values were determined for four *N*-alkyl analogs **2–5** and four aryl halide analogs **6–9** at MAO-A and MAO-B. A following *in silico* study disclosed a new adjacent compartment to the MAO-B substrate pocket defined by amino acids Tyr188, Tyr435, Tyr398, Thr399, Cys172 and Gly434. This new insight is important for the understanding of the substrate specificity of the MAO-B enzyme and will be relevant for future drug design within the field of monoamines.

Introduction

Monoamine oxidase (MAO) is a flavin adenine dinucleotide (FAD)-dependent enzyme bound to the outer mitochondrial membrane and is responsible for the oxidative deamination of monoamines such as monoaminergic neurotransmitters, dietary amines and hormones.[1,2] The enzyme exists in two isoforms, MAO-A and MAO-B, which display 70% amino acid residue identity.[3] While MAO-A is found in the brain, liver, the gastrointestinal tract and in placenta, MAO-B is only found in the brain and blood platelets.[4] Aside from differences in tissue distribution, the A/B isoforms also differ in substrate specificity. MAO-A is the predominant isoform for deamination of *e.g.* the neurotransmitters serotonin, adrenalin and noradrenalin,[4] whereas MAO-B preferentially deaminates lipophilic monoamines *e.g.* benzylamine, phenethylamine (PEA, **1**) and octylamine. The primary amines, dopamine, tyramine, kynuramine and tryptamine are common substrates for both isoforms.[5] Because the MAO enzymes are key actors in the metabolism of the monoaminergic neurotransmitters, a large number of inhibitors have been synthesized to discover novel drugs for the treatment of psychiatric and/or neurological disorders:[6,7] MAO-A inhibitors have found use as antidepressant[8,9] and anxiolytic drugs,[10,11] whereas MAO-B inhibitors are used for the treatment of Parkinson's[12,13] and Alzheimer's diseases.[7]

In contrast, a limited number of MAO substrates have been reported: Kynuramine[14] (Fig. 1), a metabolite of melatonin,[15] is a substrate for both MAO-A and B and used in *in vitro* MAO assays.[16] The substrate 1-methyl-4-phenyl-1,2,3,6-tetrahydropyridine (MPTP)[17] is converted into a neurotoxin by MAO-B[18] and has been explored as a scaffold for the synthesis of other MAO-substrates including 1-methyl-3-phenyl-2,5-dihydro-1*H*-pyrrole,[19,20] 2-methylisoindolines,[19] 4-(1-methyl-1*H*-pyrrol-2-yl)-1-(prop-2-yn-1-yl)piperidine,[21] 3,4-cyclopropyl analogs of MPTP[22] as well as 1-methyl-3-phenylpyrrolidine and the 3,4-cyclopropyl analogs hereof[23] (Fig. 1). Finally the MAO A/B substrate specificity of some neurological drugs have been investigated in order to get a more detailed understanding of the drug's pharmacokinetic properties (Sumatriptan – an anti-migraine drug[24] and Citalopram – an antidepressive drug,[25] Fig. 1).

Systematic studies of MAO-A and MAO-B substrate specificities find applications in diverse research areas such as drug discovery, development of enzyme activity assays, and new enzyme-based synthetic methodology. In contrast to the diverse and chemically complex MAO substrates depicted in

[a]*Clermont Université, Université Blaise Pascal, Institut de Chimie de Clermont-Ferrand, BP 10448, F-63000 Clermont-Ferrand, France*
[b]*CNRS, UMR 6296, ICCF, 63177 Aubière, France.*
E-mail: thierry.gefflaut@univ-bpclermont.fr; Fax: +33 473407717; Tel: +33 473407866
[c]*Department of Drug Design and Pharmacology, Faculty of Health and Medical Sciences, University of Copenhagen, Universitetsparken 2, DK-2100 Copenhagen Ø, Denmark. E-mail: lebu@sund.ku.dk; Tel: +45 35336244*
† Electronic supplementary information (ESI) available: ^{1}H NMR of compounds **3** and **4**. See DOI: 10.1039/c4ob01377h

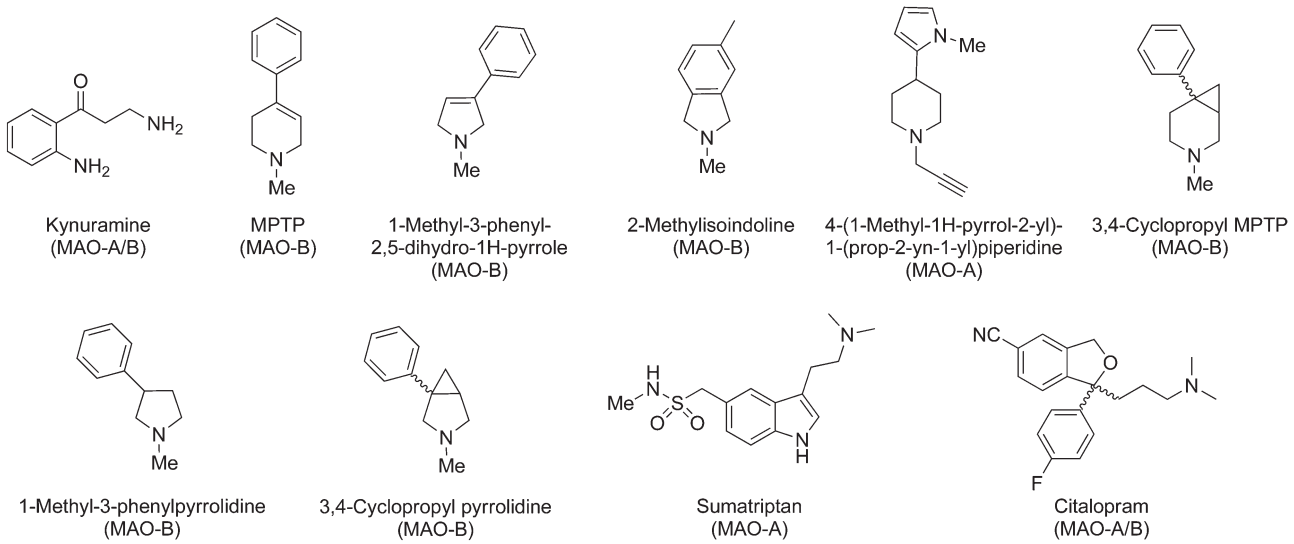

Fig. 1 Examples of MAO substrates include endogenous metabolites, synthetic compounds and drugs.

Fig. 1, phenethyl amine (PEA, **1**) is a simple arylalkyl amine which comprises the chemical features commonly found in MAO-A and MAO-B substrates. Therefore it attracted our attention to investigate the substrate specificity of two series of PEA analogs (*N*-alkyl analogs **2–5** and aryl halide analogs **6–9**, Fig. 2) at the MAO-A and MAO-B enzymes, and follow-up these results with an *in silico* study.

Results and discussion

It has previously been shown that PEA (**1**, Fig. 2) is a preferred substrate for MAO-B over MAO-A.[26] We designed two distinct series of PEA (**1**) analogs to probe the substrate specificity of the MAO-A and -B enzymes: PEA analogs **2–5** (Fig. 2) are simple aliphatic *N*-alkyl analogs increasing the chain length and bulkiness, while PEA analogs **6–9** (Fig. 2) were included in the study to explore the influence on substrate specificity of a aryl halide substituent.

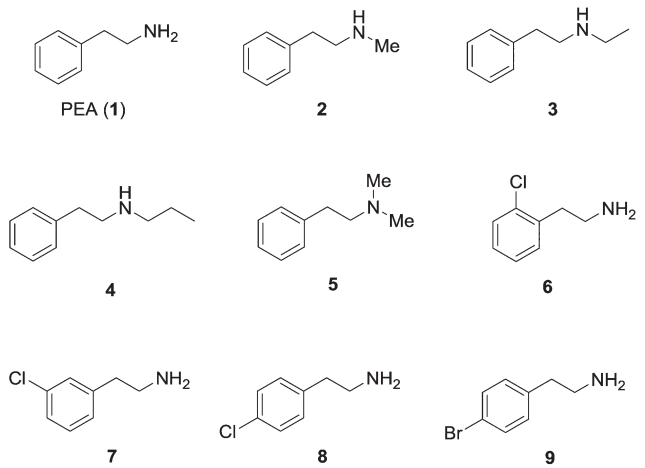

Fig. 2 Chemical structure of *N*-alkyl PEA (**1**) analogs **2–5** and aryl halide analogs **6–9**.

Synthesis of *N*-alkyl PEA (1) analogs

Whereas PEA (**1**), *N*-methyl analog **2**, *N*,*N*-dimethyl analog **5**, and aryl halide analogs **6–9** were purchased from commercial suppliers, the *N*-ethyl analog **3** and *N*-propyl analog **4** were synthesized, following a standard protocol of reductive amination of PEA (**1**) and the respective aldehyde, using $NaBH_3CN$ as the reducing agent (Scheme 1).[27] The desired secondary amines **3** and **4** were obtained in modest yields with the corresponding tertiary amines as the major side products (not shown).

MAO-A and B substrate profiling

The four *N*-alkyl PEA analogs **2–5** were then investigated as potential substrates of both MAO-A and MAO-B. Kinetic constants for the MAO-catalyzed oxidation of substrates **2–9** with O_2 were estimated using a continuous fluorescence assay based on hydrogen peroxide (H_2O_2) co-product titration. Horseradish peroxidase was used to catalyse a non-rate-limiting coupled reaction between H_2O_2 and 10-acetyl-3,7-dihydroxyphenoxazine (Amplex® Red) producing the fluorescent resorufin. This assay was previously used for the evaluation of MAO substrates or inhibitors.[28] PEA (**1**) and kynuramine were

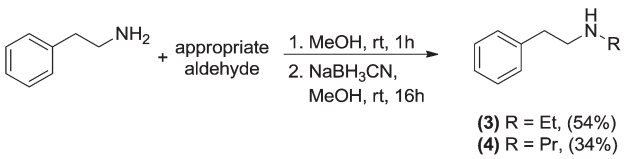

Scheme 1 Synthesis of *N*-alkyl analogs **3** and **4** *via* a one-pot reductive amination of PEA (**1**) with appropriate aldehydes.

Table 1 MAO-A and -B substrate activities of kynuramine, PEA (**1**), *N*-alkyl analogs **2–5**, and aryl halide analogs **6–9**. K_m in [μM], k_{cat} in [min^{-1}] and k_{cat}/K_m in [min^{-1} μM^{-1} × 1000]

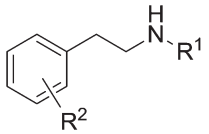

1-9

			MAO-A			MAO-B		
Cmpd no.	R^1	R^2	K_m	k_{cat}	k_{cat}/K_m	K_m	k_{cat}	k_{cat}/K_m
Kynuramine	—	—	378 ± 17.3	7.90 ± 0.22	20.9 ± 1.1	37.3 ± 1.4	1.36 ± 0.02	36.4 ± 1.5
PEA, **1**	H	H	4550 ± 549	9.63 ± 1.09	2.1 ± 0.4	7.0 ± 0.4	3.12 ± 0.10	444 ± 27.6
2	Me	H	402 ± 9.9	5.84 ± 0.10	14.5 ± 0.4	5.4 ± 0.4	2.25 ± 0.07	419 ± 32.2
3	Et	H	n.s.	n.s.	n.s.	343 ± 22.6	2.20 ± 0.10	6.4 ± 0.5
4	Pr	H	n.s.	n.s.	n.s.	515 ± 61.9	1.26 ± 0.12	2.4 ± 0.4
5	Me, Me	H	n.s.	n.s.	n.s.	112 ± 15.1	0.96 ± 0.03	8.5 ± 1.2
6	H	*o*-Cl	70.9 ± 2.5	16.8 ± 0.27	237 ± 9.0	2.9 ± 0.2	1.85 ± 0.07	638 ± 45.9
7	H	*m*-Cl	24.3 ± 1.4	5.21 ± 0.09	214 ± 13.1	3.2 ± 0.3	1.97 ± 0.14	623 ± 68.1
8	H	*p*-Cl	152 ± 8.1	1.87 ± 0.06	12.3 ± 0.8	2.4 ± 0.2	3.41 ± 0.12	1430 ± 117
9	H	*p*-Br	178 ± 14.0	1.46 ± 0.07	8.2 ± 0.7	2.3 ± 0.2	3.84 ± 0.15	1690 ± 147

n.s.: not substrate.

included as reference substrates, and results summarized in Table 1. As *N*-alkyl PEA analogues **2–5** release simple *N*-alkylamines upon MAO-catalyzed oxidation and hydrolysis, the MAO activity with *N*-methyl-, *N*-ethyl-, *N*-propyl- and *N*,*N*-dimethylamine was needed to be addressed. For both MAO-A and MAO-B isoforms, no activity was detected with any of these four *N*-alkyl amines.

In summary for MAO-A activity, the *N*-Me analog **2** displays a 10-fold increase in affinity (K_m) compared to PEA (**1**). On the other hand, the turnover number (k_{cat}) for **2** is roughly 50% lower. Elongation of the *N*-alkyl chain (*N*-ethyl analog **3** and *N*-propyl analog **4**) resulted in complete loss of MAO-A activity. Furthermore, the more bulky *N*,*N*-dimethyl analog **5** was not a substrate for the MAO-A enzyme. Exploration of an aryl halide substituent, analogs **6–9**, resulted in a 25–200-fold increase in affinity for MAO-A. The effect on k_{cat} spanned from a 2-fold increase (*o*-Cl, compound **6**), over a 2-fold decrease (*m*-Cl, compound **7**) to a 6-fold decrease (*p*-Cl and *p*-Br, compound **8** and **9**) (Table 1). Overall, compared to PEA, **6** and **7** were 100-fold better substrates for MAO-A, while **8** and **9** were only 4–6 fold better.

The activity profile observed for MAO-B with the substrate series **2–9** was highly different. The activity measured with the *N*-methyl analog **2** was comparable with that of **1** both with respect to K_m and k_{cat}. Extending the *N*-alkyl chain to an *N*-ethyl group, compound **3**, gave a significant (50-fold) drop in affinity (K_m) for MAO-B. With a further extension to *N*-propyl, compound **4**, a 70-fold drop in K_m was observed in comparison with **1**. On the other hand, *N*,*N*-dimethyl analog **5** displayed only a 15-fold drop in affinity (K_m = 112 μM) as compared with **1**. For all four analogs **2–5**, the turnover number, was determined to be within the same range (k_{cat} = 0.96–2.25 min^{-1}) – slightly lower than for **1**. The effect of an arylic chloride or bromide, analogs **6–9**, was manifested in a 2 to 3-fold increase in affinity (K_m), while the turnover number was roughly the same (k_{cat}) in comparison to **1**. In summary, a chloride in either the *o*- or *m*-position gave little change in activity, whereas a halide in the *p*-position improved MAO-B activity by 4-fold.

The comparison of the activities of the two isoforms MAO-A and B towards this substrate series confirms that MAO-B shows a much stronger affinity for PEA, and analogs thereof, than MAO-A. A K_m ratio of 650 was obtained for PEA, whereas, the different analogues **2** and **6–9** showed a drop in selective affinity with K_m ratio ranging from 7.6 to 77. Conversely, higher k_{cat} values were measured with MAO-A for several compounds. *N*-Methyl analog **2**, *m*-chloro derivative **7** and PEA itself displayed a 2 to 3 fold higher value, whereas the *o*-chloro PEA derivative **6** showed a nine fold higher k_{cat} value for MAO-A compared to MAO-B. However, the k_{cat} values which are calculated from protein content independently for each enzyme should be compared with some carefulness, even though commercial MAO-A and MAO-B batches are reported to be of high purity and to display the same level of activity in the microsomal expression system. Besides, regarding the k_{cat}/K_m values, compounds **6** and **7** clearly appear as good substrates for both enzymes, much better than kynuramine which is commonly used as a non-selective substrate in MAO assays. In addition, the *p*-bromo derivative **9**, displays a high selectivity for MAO-B with k_{cat}/K_m 200 times higher compared to MAO-A. Although this selectivity ratio is similar to that observed with PEA, compound **9** shows a 4 times higher activity and constitute therefore a new valuable substrate for MAO-B selective assays.

In regard to already published studies on the role of MAO-A and MAO-B enzymes in drug metabolism, the results of *N*-alkyl PEA analogs **2–5** are intriguing. It has been shown, that the anti-migraine drug Sumatriptan, which comprises an

N,*N*-dimethyl amine moiety, is metabolized primarily by MAO-A.[24] Furthermore, it has been shown that the antidepressant drug Citalopram, which also comprises an *N*,*N*-dimethyl amine moiety, is metabolized by both the MAO-A and MAO-B enzymes.[2]

Modeling. The MAO-B enzyme has previously been crystallized with covalently bound FAD (PDB code: 2VRL).[29] In the proximity of the covalently bound FAD molecule the *substrate binding pocket* has been identified and is of lipophilic nature (Fig. 3). In connection hereto, a second pocket has been defined and following named the *entrance pocket*. The *substrate* and *entrance* pockets are narrowed in at the site of their joining by the side chains of amino acid residues Leu171, Tyr326 and Ile199, although the latter is in its open form.[29]

Two distinct mechanisms have been suggested for the catalytic action of the MAO-A and MAO-B enzymes; a radical reaction and a polar nucleophilic mechanism.[2] While the latter is the most commonly accepted one, details on nitrogen protonation states are disputed.[2] Earlier it has been proposed that the substrate is at its free amine form when it is directed to the substrate pocket. However, based on the fact that π–cation interactions are of stabilizing nature in contrast to repulsive π-electron–free-amine interactions, the amine substrates likely remain protonated at the stage of entrance and are directed to the substrate pocket by exchanging π–cation interactions with the aromatic residues in the entrance and substrate pockets. Approaching the FAD, the ammonium group protonates *N*(5) preceding its nucleophilic attack on C(4a) to form key intermediate A (Scheme 2). This covalently-bound FAD-substrate complex was selected as the starting point for a computational searching for binding mode of the active substrates reported herein.

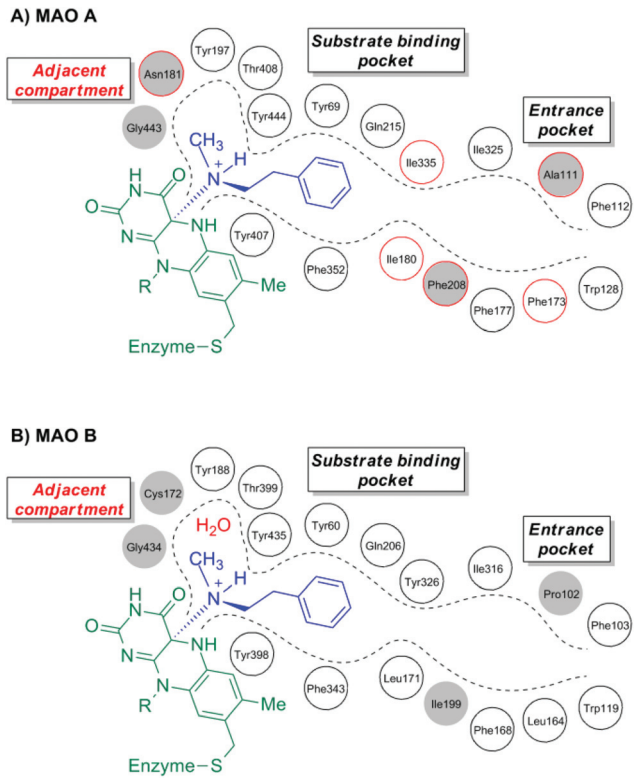

Fig. 3 Amino acid residues forming the entrance pocket, the substrate binding pocket and the newly discovered adjacent compartment of the MAO-A/B enzymes. Filled circles designate residue backbone as pocket wall and unfilled circles designate residue side chain as pocket wall. Red circles designate residue of differentiation between MAO-A and MAO-B. (A) MAO-A amino acid residue alignment onto X-ray structure of MAO-B (2VRL). (B) X-Ray structure of MAO-B (2VRL) with covalently-bound FAD in green and covalently bound protonated substrate *N*-methyl-phenethylamine (**2**) in blue.

While X-ray crystal structure determination of an enzyme-bound substrate is not possible due to its transient nature, the crystal structure of covalently-bound inhibitor, benzylhydrazine with MAO-B (PDB code: 2VRL), has been reported[29] and was selected as a suitable starting template for the modeling study. Firstly, structural changes were made to the FAD-ligand complex as to represent key intermediate A (Scheme 2) comprising the appropriate *N*-substituent. For analogs **2–4** both geometries of the positively charged nitrogen were built and modeled independently, while the symmetry of dimethyl analog **5** allowed for building of only one. Each structural complex was submitted to a LowModeMD simulation and the sample of conformers was examined. Overall, analogs **2–5** were well-accommodated by the MAO-B enzyme.

In details, the *in silico* study concluded that the *N*-alkyl moieties reach into an adjacent hydrophobic compartment defined by the side chains of amino acids Tyr188, Tyr435, Tyr398 and Thr399, and backbone carbonyl groups of Cys172 and Gly434 (Fig. 3B). It is noteworthy that a water molecule is located in this compartment and it engages in a hydrogen bonding interaction with the carbonyl group of Cys172. Thus, for *N*-alkyl group larger than methyl this water molecule must be displaced. Moreover, the *N*-phenethyl groups are well-fitted in the substrate binding pocket. For analogs **2–4** the major difference between their two protonated states is the orientation of the *N*-proton, which engages in π–cation interactions with residues Tyr398 or Tyr435. We propose that the protonated state, which forms π–cation interaction with Tyr435 (Fig. 3B and 4) is favorable due to the spatial orientation of the α-hydrogen atom, as this is believed to undergo *N*(5)-base catalyzed elimination (Scheme 2, step c).

Positively charged quaternary amine **5** revealed similar binding modes as described above for analogs **2–4**, but orienting one *N*-methyl group towards Tyr435 or Tyr398. The spatial orientation of the phenethyl moiety is similar but the conformation of the methyl groups suggests that the conformer in which the *N*-methyl group points towards Tyr435 is favored due to the *N*(5)-base catalyzed elimination of α-hydrogen atom (Scheme 2, step c). The 20-fold loss in affinity (compound **2** *vs.* compound **5**) could be due to a possible steric clash between the one *N*-methyl group of **5** and Tyr435.

To investigate the observed differences in binding affinity of **2–5** at MAO-A and MAO-B, the amino acid sequence of human MAO-A was aligned with the X-ray structure of MAO-B used in the *in silico* study (2VRL) (Fig. 3A). Only the Cys172

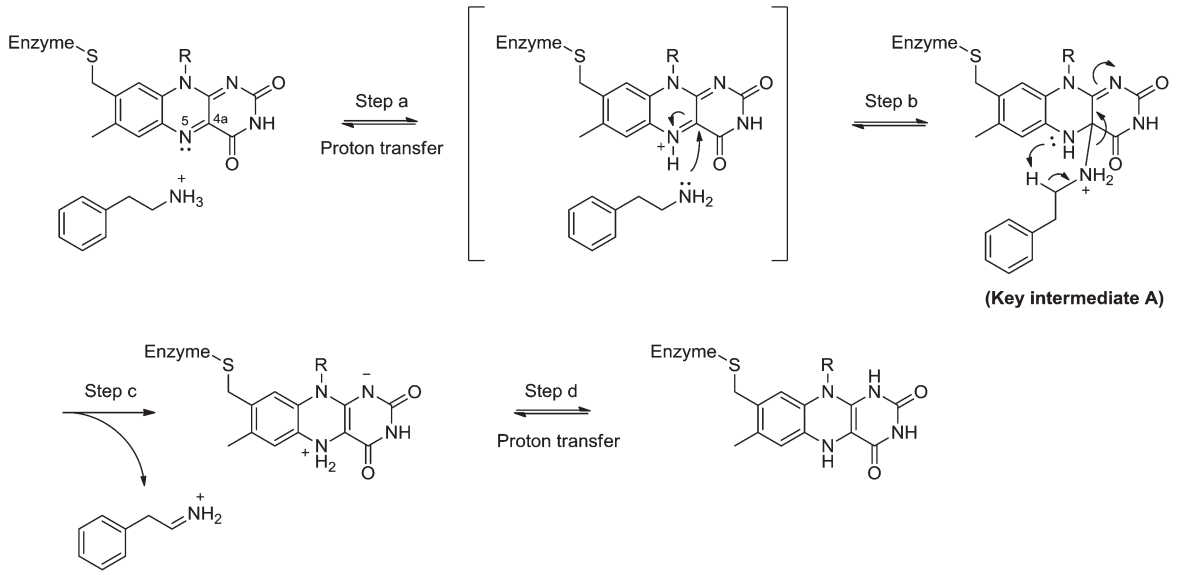

Scheme 2 Suggested polar nucleophilic mechanism for MAO-B-catalyzed oxidation of amines.

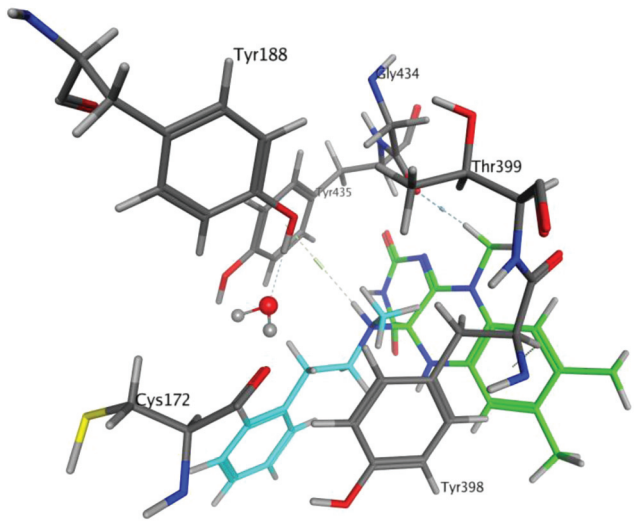

Fig. 4 Amino acids occluding the adjacent compartment in MAO-B. Covalently-bound FAD in green with covalently-bound protonated substrate *N*-methyl-phenethylamine (**2**) in blue. Key water molecule in type code.

residue of MAO-B is altered to an Asn181 in MAO-A. Indeed Asn181 comprises a more bulky side chain, but since it is the backbone carbonyl group which defines the adjacent compartment, the chemical nature of the side chain must have little direct involvement. However, the water molecule found in the X-ray of MAO-B is believed also to be present in MAO-A. Herein it could be more tightly bound due to the before described difference in amino acid residue. Displacement for larger *N*-alkyl groups than methyl would then be disfavored, rendering such *N*-alkyl analogs inactive as substrates for MAO-A.

The *ortho* and *meta* aryl positions direct substituents into conserved space between MAO-A and MAO-B (Fig. 3) and a chloride increases affinity in both cases. However, both *para* aryl chloride and bromide are disfavored for MAO-A, but well-accepted for MAO-B. These difference are likely to be explained by the distinct amino acid residues defining the doorstep between the substrate pocket and the entrance pocket of MAO-A and MAO-B (Fig. 3, MAO-B → MAO-A: Leu171 → Ile180, Ile199 → Phe208 and Tyr326 → Ile335).

Conclusion

In conclusion, the MAO-A and MAO-B substrate specificity profile was studied for two series of PEA (**1**) analogs: for the *N*-alkyl PEA series, analogs **2–5**, an *N*-methyl group, compound **2**, was tolerated by both isoforms. On increasing the alkyl chain length or bulkiness complete loss of enzymatic activity at MAO-A was observed while the affinity for MAO-B was lowered by 20–70 fold. The series comprising analogs with an aryl halide substituent, compounds **6–9**, showed that the position of substitution has a strong influence on isoform preference, with the *para* position favoring substrate specificity towards the MAO-B isoform. An *in silico* study suggested that the *N*-alkyl substituents occupy an adjacent compartment to the substrate pocket defined by amino acids Tyr188, Tyr435, Tyr398, Thr399, Cys172 and Gly434 (Fig. 3B and 4). This new insight is relevant to the understanding of MAO-B substrate specificity and will be of importance to future drug design within the field of monoamines.

Experimental section

Chemistry

Chemicals and reagents purchased from commercial suppliers were used without further purification. Solvents were of HPLC

quality and used as received. Evaporation *in vacuo* was performed on a rotary evaporator at approx. 40 °C (pressure: 20 mbar). TLC was performed using silica gel 60 F_{254} aluminium sheets. The plates were visualized in under UV light (254 nm) followed by staining with $KMnO_4$ or 0.5% ninhydrin in EtOH. ^{1}H NMR (300 MHz) and ^{13}C NMR (75 MHz) spectra were recorded on a Varian Mercury Plus and on a Varian Gemini 2000 instrument, respectively, using deuterated solvents as internal references. Chemical shifts (δ) are given in ppm and coupling constants (J) in Hertz. LC-MS was recorded on an Agilent 1200 series solvent delivery system equipped with an Agilent 6400 series triple quadrupole mass spectrometer (ESI) using a 10→90% MeCN gradient in H_2O containing 0.05% HCOOH.

***N*-Ethyl-2-phenethylamine (3).** Acetaldehyde (0.20 mL, 3.5 mmol, 1.00 equiv.) was added to a stirred solution of PEA (**1**) (1.34 mL, 1.29 g, 10.6 mmol, 3.03 equiv.) in dry MeOH (30 mL) at 0 °C under a N_2 atmosphere. The reaction mixture was stirred for 30 min at 0 °C and for 1.5 hours at rt. $NaBH_3CN$ (245 mg, 3.9 mmol, 1.11 equiv.) was added and the reaction mixture was stirred at rt for 28 hours. After concentration *in vacuo*, the crude product was purified by flash chromatography using isocratic EtOAc–MeOH–Et_3N (10 : 1 : 0.1). This afforded the titled compound (287 mg, 54%) as a colorless oil. R_f 0.28 (EtOAc–MeOH–Et_3N 10 : 1 : 0.1). ^{1}H NMR (D_2O) δ 7.40 − 7.25 (m, 5H), 3.25 (t, J = 7 Hz, 2H), 3.05 (q, J = 7 Hz, 2H), 2.95 (t, J = 7 Hz, 2H), 1.18 (t, J = 7 Hz, 3H). ^{13}C NMR ($CDCl_3$) δ 140.5, 129.0, 128.8, 126.5, 51.5, 44.4, 36.9, 15.7. MS (m/z) calcd for $C_{10}H_{15}N$ $[M + H]^+$ 150.1, found: 150.2.

***N*-Propyl-2-phenethylamine (4).**[27] Propionaldehyde (0.3 mL, 5.2 mmol, 1.00 equiv.) was added to a stirred solution of PEA (**1**) (2.0 mL, 1.92 g, 15.5 mmol, 2.98 equiv.) in dry MeOH (45 mL) at rt under a N_2 atmosphere. The reaction mixture was stirred for 1 hour at rt. $NaBH_3CN$ (357 mg, 5.7 mmol, 1.10 equiv.) was added and the reaction mixture was stirred at rt for 5 hours. The reaction mixture was concentrated *in vacuo*. H_2O (25 mL) was added and the solution was extracted with DCM (3 × 30 mL). The combined organic phases were washed with H_2O (30 mL) and brine (30 mL). The organic phase was dried over anhydrous Na_2SO_4. After concentration *in vacuo*, the crude product was purified by flash chromatography using isocratic EtOAc–MeOH–Et_3N (10 : 1 : 0.1) and the product was further distilled under reduced pressure (b.p. 168 − 170 °C/250 mmHg) to afford the titled compound (232 mg, 34%) as a colorless oil. R_f 0.14 (EtOAc–MeOH–Et_3N 10 : 1 : 0.1). ^{1}H NMR ($CDCl_3$) δ 7.30 − 7.16 (m, 5H), 2.91 − 2.85 (m, 2H), 2.83 − 2.77 (m, 2H), 2.58 (t, J = 7.5 Hz, 2H), 1.48 (sextet, J = 7.5 Hz, 2H), 0.89 (t, J = 7.5 Hz, 3H). ^{13}C NMR ($CDCl_3$) δ 140.2, 128.8, 128.5, 126.3, 51.9, 51.4, 36.6, 23.3, 11.9. MS (m/z) calcd for $C_{11}H_{17}N$ $[M + H]^+$ 164.1, found: 164.2.

MAO-A and B substrate assays

Human monoamine oxidase A and B (MAO-A and MAO-B) supersomes were purchased from BD Biosciences. Amplex red® was purchased from Invitrogen. Horseradish peroxidase (HRP) was purchased from Sigma-Aldrich. The batches (0.5 mL, 2.5 mg) were thawed rapidly in a 37 °C water bath upon arrival, aliquoted and quickly refrozen to −80 °C until further use. Before use, MAOs were thawed and then diluted to obtain a 0.16 mg mL^{-1} solution in 50 mM phosphate buffer pH = 7.4. A 2 mM solution of Amplex red was prepared in 50 mM phosphate buffer pH = 7.4, 10% v/v DMSO. A 4 μg mL^{-1} solution of HRP was prepared in 50 mM phosphate buffer pH = 7.4. A mixed solution of 0.5 mM Amplex red®, 1 μg mL^{-1} HRP in 50 mM phosphate buffer pH = 7.4, 2.5% v/v DMSO, was prepared just before use from the two previous solutions. 2 mM solutions of the various amino substrates were prepared in 50 mM phosphate buffer pH = 7.4, 4% v/v DMSO. 1 μM to 2 mM amino substrates solutions were then prepared by dilution in the same buffer.

MAO activity fluorescence assays was automated on a monochromator-based fluorescence microplate reader (Safire™, Tecan) using 96-well fluorescence microplates, incubated at 37 °C in the dark. The reaction mixture was composed of 20 μL of MAO solution, 80 μL of the mixed solution containing HRP and Amplex red®, and 100 μL of substrate solution. Enzymatic reactions were initiated with the substrate and monitored over 30 min by fluorimetry using excitation at λ = 563 ± 10 nm and detection at λ = 587 ± 10 nm.

For each substrate, kinetic parameters were determined using at least 7 different concentrations close to the estimated K_m value. Each experiment was reproduced three times using substrate mother solutions prepared independently. Maximal slope were measured within the first 15 min (RFU min^{-1}) and converted to initial reaction velocities (μM H_2O_2 min^{-1}), using a standard curve obtained with titrated H_2O_2 solutions under the same assay conditions. Kinetic parameters and standard errors were calculated from the Hanes–Woolf plot according to the least-squares method and Gauss's error propagation law.

Modeling

The comprehensive molecular modeling suite MOE (version 2011.10, Chemical Computing Group) running on a Windows 7 Professional 32 bit PC platform was used. The force field PFROSST was used with solvation set to *distance*. For each analog **2–5**, PDB file 2VRL was imported and altered chemically to represent key intermediate A with the appropriate *N*-substituent. In cases where two protonation states were possible, both were built and considered independently. Each generated structural complex was first submitted to the LigX command to restrain atoms further away than 8 Å from the ligand (standard setup). Subsequently a conformational search by LowModeMD (a short molecular dynamics simulation using velocities with little kinetic energy on the high-frequency vibrational modes[30]) was carried out using standard setup with the following changes: RMS gradient = 0.1 and Energy window = 1000.

Alignment of human MAO-A amino acid sequence onto MAO-B (2VRL) was done by standard setup of alignment function in MOE (hMAO-A: 527).

Abbreviations

FAD	Flavin adenine dinucleotide
MAO	Monoamine oxidase
MPTP	1-Methyl-4-phenyl-1,2,3,6-tetrahydropyridine
PAA	2-Phenylacetaldehyde
PEA	Phenethylamine

References

1 J. Wouters, *Curr. Med. Chem.*, 1998, **5**, 137–162.
2 D. E. Edmondson, A. Mattevi, C. Binda, M. Li and F. Hubálek, *Curr. Med. Chem.*, 2004, **11**, 1983–1993.
3 A. W. Bach, N. C. Lan, D. L. Johnson, C. W. Abell, M. E. Bembenek, S. W. Kwan, P. H. Seeburg and J. C. Shih, *Proc. Natl. Acad. Sci. U. S. A.*, 1988, **85**, 4934–4938.
4 M. Da Prada, R. Kettler, H. H. Keller, A. M. Cesura, J. G. Richards, J. Saura Marti, D. Muggli-Maniglio, P. C. Wyss, E. Kyburz and R. Imhof, *J. Neural Transm., Suppl.*, 1990, **29**, 279–292.
5 L. W. Elmer and J. M. Bertoni, *Expert Opin. Pharmacother.*, 2008, **9**, 2759–2772.
6 A. Bolasco, S. Carradori and R. Fioravanti, *Expert Opin. Ther. Pat.*, 2010, **20**, 909–939.
7 M. Bortolato, K. Chen and J. C. Shih, *Adv. Drug Delivery Rev.*, 2008, **60**, 1527–1533.
8 J. D. Amsterdam and J. Shults, *J. Affective Disord.*, 2005, **89**, 183–188.
9 R. Amrein, W. Hetzel, M. Stabl and W. Schmid-Burgk, *Int. Clin. Psychopharmacol.*, 1993, **7**, 123–132.
10 M. A. Jenike, O. S. Surman, N. H. Cassem, P. Zusky and W. H. Anderson, *J. Clin. Psychiatry*, 1983, **44**, 131–132.
11 M. Cyr and M. K. Farrar, *Ann. Pharmacother.*, 2000, **34**, 366–376.
12 A. M. Cesura and A. Pletscher, *Prog. Drug Res. Fortschr. Arzneimittelforsch. Prog. Rech. Pharm.*, 1992, **38**, 171–297.
13 J. Knoll, *Neurobiology*, 2000, **8**, 179–199.
14 H. Weissbach, T. E. Smith, J. W. Daly, B. Witkop and S. Udenfriend, *J. Biol. Chem.*, 1960, **235**, 1160–1163.
15 R. Hardeland, D.-X. Tan and R. J. Reiter, *J. Pineal Res.*, 2009, **47**, 109–126.
16 I. Mahmood, S. H. Neau and W. D. Mason, *J. Pharm. Biomed. Anal.*, 1994, **12**, 895–899.
17 J. Lee and A. Ziering, *J. Org. Chem.*, 1947, **12**, 885–893.
18 M. O. Ogunrombi, S. F. Malan, G. Terre'Blanche, K. Castagnoli, N. Castagnoli, J. J. Bergh and J. P. Petzer, *Life Sci.*, 2007, **81**, 458–467.
19 Y. X. Wang, S. Mabic and N. Castagnoli, *Bioorg. Med. Chem.*, 1998, **6**, 143–149.
20 Y. Lee, K.-Q. Ling, X. Lu, R. B. Silverman, E. M. Shepard, D. M. Dooley and L. M. Sayre, *J. Am. Chem. Soc.*, 2002, **124**, 12135–12143.
21 P. Bissel, M. C. Bigley, K. Castagnoli and N. Castagnoli, *Bioorg. Med. Chem.*, 2002, **10**, 3031–3041.
22 J. M. Rimoldi, S. G. Puppali, E. Isin, P. Bissel, A. Khalil and N. Castagnoli, *Bioorg. Med. Chem.*, 2005, **13**, 5808–5813.
23 A. Pretorius, M. O. Ogunrombi, H. Fourie, G. Terre'blanche, N. Castagnoli, J. J. Bergh and J. P. Petzer, *Bioorg. Med. Chem.*, 2010, **18**, 4111–4118.
24 C. M. Dixon, G. R. Park and M. H. Tarbit, *Biochem. Pharmacol.*, 1994, **47**, 1253–1257.
25 B. Rochat, M. Kosel, G. Boss, B. Testa, M. Gillet and P. Baumann, *Biochem. Pharmacol.*, 1998, **56**, 15–23.
26 K. Orito, A. Horibata, T. Nakamura, H. Ushito, H. Nagasaki, M. Yuguchi, S. Yamashita and M. Tokuda, *J. Am. Chem. Soc.*, 2004, **126**, 14342–14343.
27 M. Zhou and N. Panchuk-Voloshina, *Anal. Biochem.*, 1997, **253**, 169–174.
28 C. Binda, J. Wang, M. Li, F. Hubalek, A. Mattevi and D. E. Edmondson, *Biochemistry*, 2008, **47**, 5616–5625.
29 F. Hubálek, C. Binda, A. Khalil, M. Li, A. Mattevi, N. Castagnoli and D. E. Edmondson, *J. Biol. Chem.*, 2005, **280**, 15761–15766.
30 P. Labute, *J. Chem. Inf. Model.*, 2010, **50**, 792–800.